THE ROLE OF OCEAN COLOR IN THE VARIABILITY OF THE TROPICAL PACIFIC

Whit Anderson[1,2] Anand Gnanadesikan[2], and Andrew Wittenberg[2]

[1] AOS Program, Princeton University, Princeton NJ, USA
[2] NOAA Geophysical Fluid Dynamics Laboratory, Princeton NJ, USA

Abstract

The role of the penetration length scale of shortwave radiation into the surface ocean and its impact on tropical Pacific variability is investigated with a fully coupled ocean, atmosphere, land and ice model. Previous work has shown that removal of all ocean color results in a system that tends strongly towards an El Nino state. Results from a suite of surface chlorophyll perturbation experiments show that the mean state and variability of the tropical Pacific is highly sensitive to the concentration and distribution of ocean chlorophyll. Setting the near oligotrophic regions to contain optically pure water warms the equator in the mean and *suppresses* variability in the western tropical Pacific. Doing the same in the shadow zones of the tropical Pacific also warms the equator but *enhances* the variability. These results suggest that non-local and coupled ocean-atmosphere dynamics control the variability and play a role in determining the mean state of the tropical Pacific. Potential mechanisms that explain the role of ocean color in the tropical Pacific variability are explored and discussed.

Models and experiments

The ocean model used in this study is the Hallberg Isopycnal Model (HIM) [Hallberg, 2005]. HIM is run at 1 resolution in latitude and longitude, with meridional resolution equatorward of 30 becoming progressively finer, such that the meridional resolution is 3/8 at the equator. The ocean mixed layer is represented with a refined bulk mixed layer model [Hallberg, 2003]. HIM is coupled to the atmosphere, land and ice components used in the GFDL global coupled climate model [Delworth et al., 2006].

We use the model for shortwave penetration into the water column proposed by Manizza et al. [2005] which is based on the data of Morel [1988]. The scheme parameterizes shortwave extinction in terms of near-surface chlorophyll-a concentration. It is consistent with the Morel [1988] scheme at the lower limit of its validity. The Manizza scheme has a deeper clear-water reference than previous algorithms, resulting in shortwave-induced heating at depths well beyond 100 m. This heating becomes significant when integrated over decadal and larger time-scales.

Five global simulations are run using the simulation protocol for the 1990 control runs with the GFDL coupled climate model [Delworth et al., 2006] in which aerosols and greenhouse gasses are held constant. Initial conditions for all coupled simulations are identical and are based on those described in Delworth et al. [2006]. One simulation (Green) uses the SeaWiFS monthly composite chlorophyll-a from 1998-2004 to determine the shortwave absorption profile. In a second simulation (Blue), chlorophyll-a is set to zero to emulate the absorption profile of optically pure water. These experiments were run for 100 years, long enough to establish surface biases [Gnanadesikan et al., 2006].

To investigate the importance of equatorial and near equatorial regions, three additional coupled simulations with modification to Pacific chlorophyll monthly mean concentrations are run: one where chlorophyll concentration falling between latitudinal bands 5 N and 5 S in the Pacific are set to zero (Noequ); a second where chlorophyll concentrations falling below 0.2 mg/m3 in the Pacific are set to zero (Minus0.2); and a third where concentrations above 0.2 mg/m3 are set to zero (Plus0.2) (Fig. 1b).

Results and Discussion

The mean state differences of Blue minus Green display patterns of a an El Niño in the ocean as well as the atmosphere (Figs 2a-3a). By removing the ocean color a warming of Pacific cold tongue is induced. This is accompanied by a zonal shift in precipitation consistent with a strong ENSO warm event.

The three chlorophyll perturbation experiments showed this response with varying degrees of strength and spatial distribution (Figs 2b-d and 3b-d). Interestingly, the Noequ run displayed the weakest response.

The variability of the coupled model appears to be sensitive to ocean color as well (Fig. 4). The Blue has little power in the annual or ENSO spectral bands when compared to Green. Minus0.2 has a similar response in the ENSO band as Blue. Plus0.2 alone has an increase of power in ENSO bands. Noequ (not shown) had spectral characteristics very similar to Green.

Previous studies have shown that ocean color can have a impact on tropical variability [Murtugudde et al. 2002, Lengange 2007 and Wetzel 2007]. In explaining this imapct these studies have focused on the mean state of the Pacific tropical thermocline. Examining the mean thermocline depth in these experiments lead us to believe that there

are other drivers in the change in variability (Fig. 4). The changes in Pacific tropical variability are not consistent with the changes in slope and mean depth of the mean thermocline (Fig. 5).

To investigate other possible mechanisms for changes in the varibility we focused on the primary ENSO feedbacks (the orange and black cartoon below). Could we explain the variability differences as a function of the differences in: differences in radiative feedbacks? SST expression of ENSO? wind response to SST anomalies? thermocline adjustment/response to wind anomalies? or changes of SST through perturbations in upwelling strength?

In the table above the feedback schematic we address the first mechanism, examining correlation and regression strengths between heat flux and SST (left) and shortwave and SST (right). The heat flux feedback is consistent with the difference between Blue and Green, but does not explain why the other runs differ.

Next we look at how ENSO oscillations manifest in SST among the various experiments. Figure 6 shows the first empirical orthogonal function (EOF) for the detrended SST (normalized to unit amplitude). While there are subtle differences, the overall character of the ENSOs appear the same. The changes in variability do not appear to be a result in a change in SST spatial response.
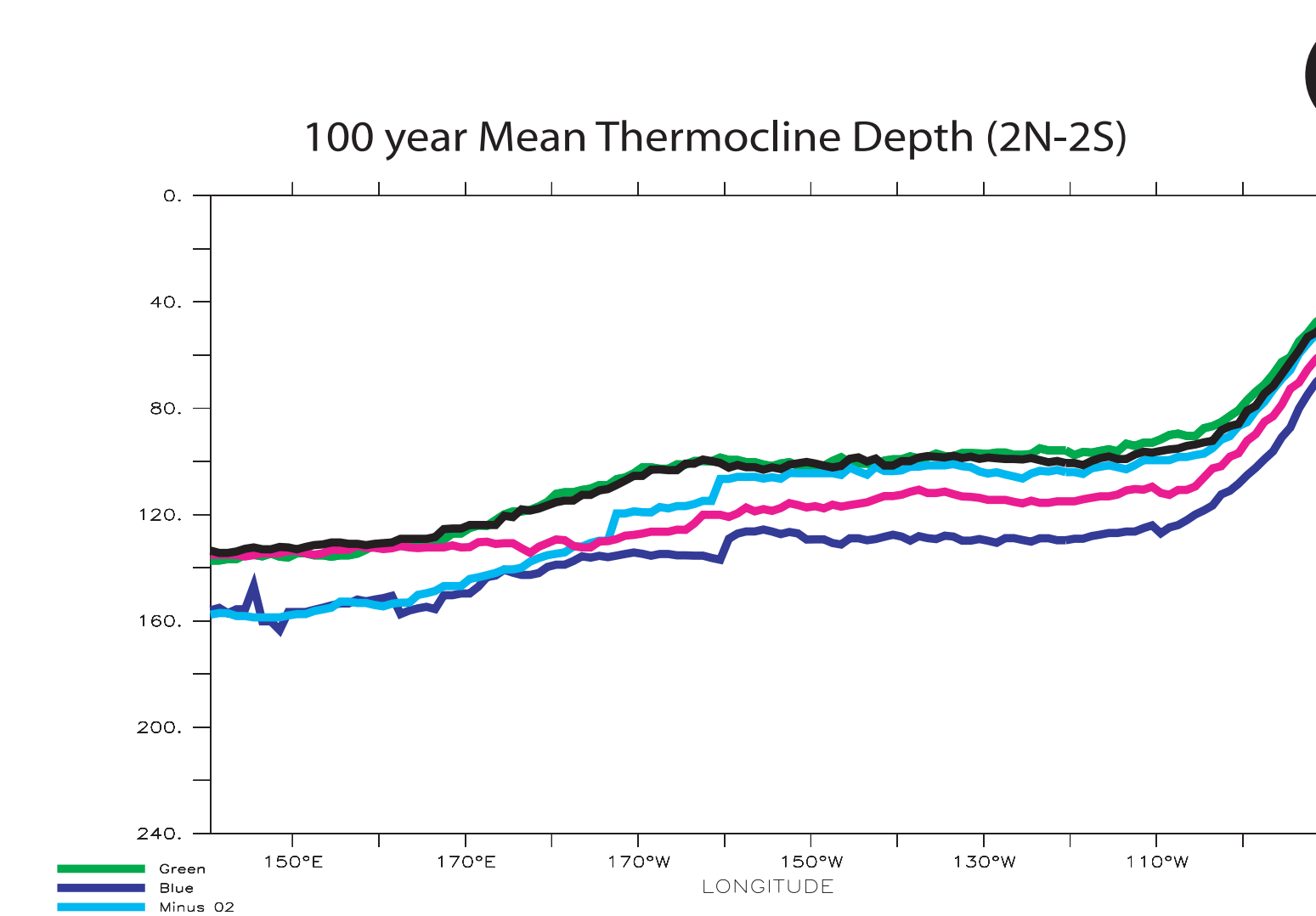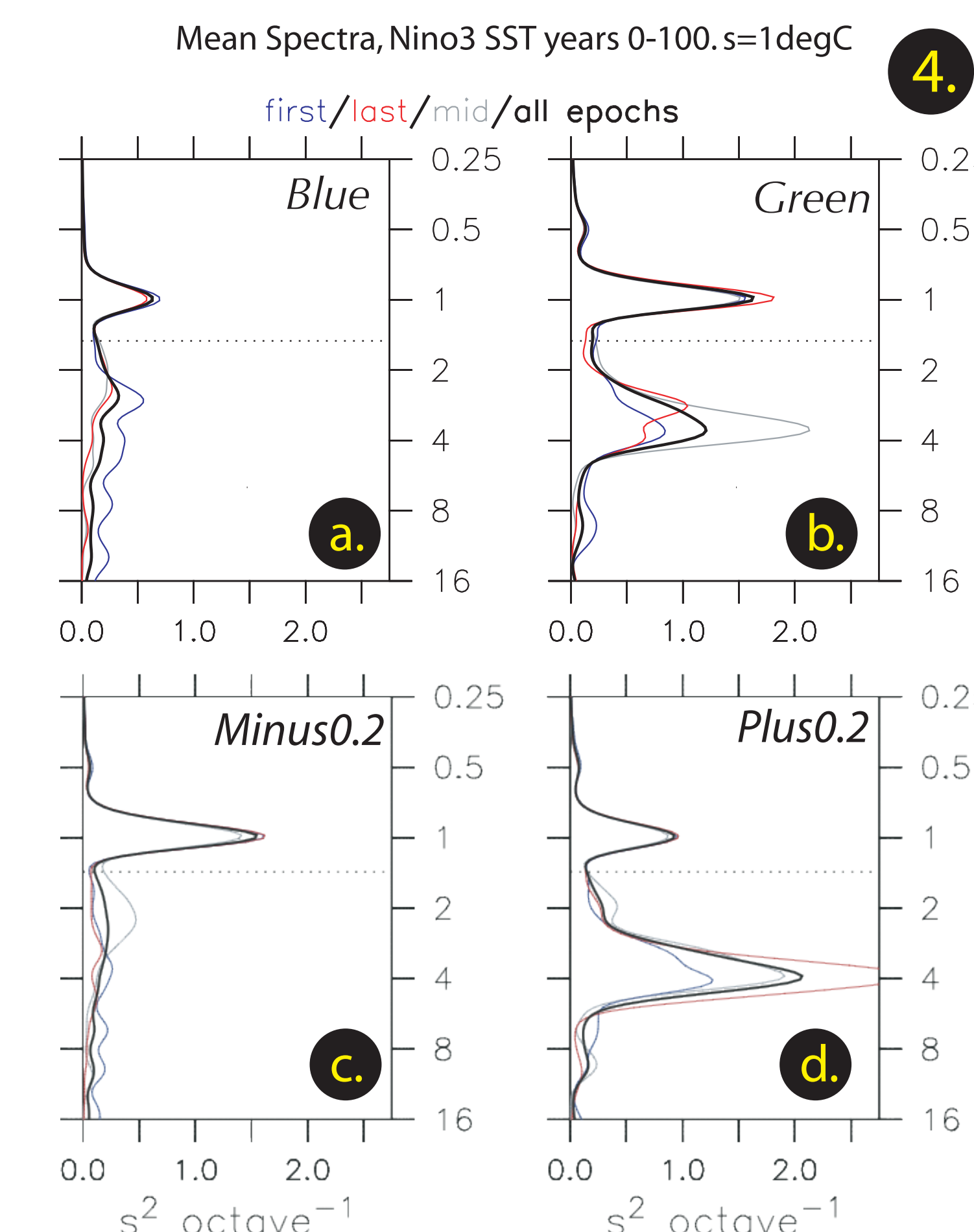
	Heat flux-SST		Shortwave-SST	
	Corr.	Regr.	Corr.	Regr.
Green	-0.91	-11.00	-0.58	-2.76
Blue	-0.89	-21.05	-0.85	-13.14
Minus02	-0.79	-11.77	-0.58	-4.77
Plus02	-0.94	-14.99	-0.73	-5.83

SST

EOF pattern different?

Response/correlation different?

Q

Radiative feedbacks?

Primary ENSO feedbacks

Z_{20} τ^x

Regression pattern different?

Amplitude of Kelvin/Rossby Wave response?
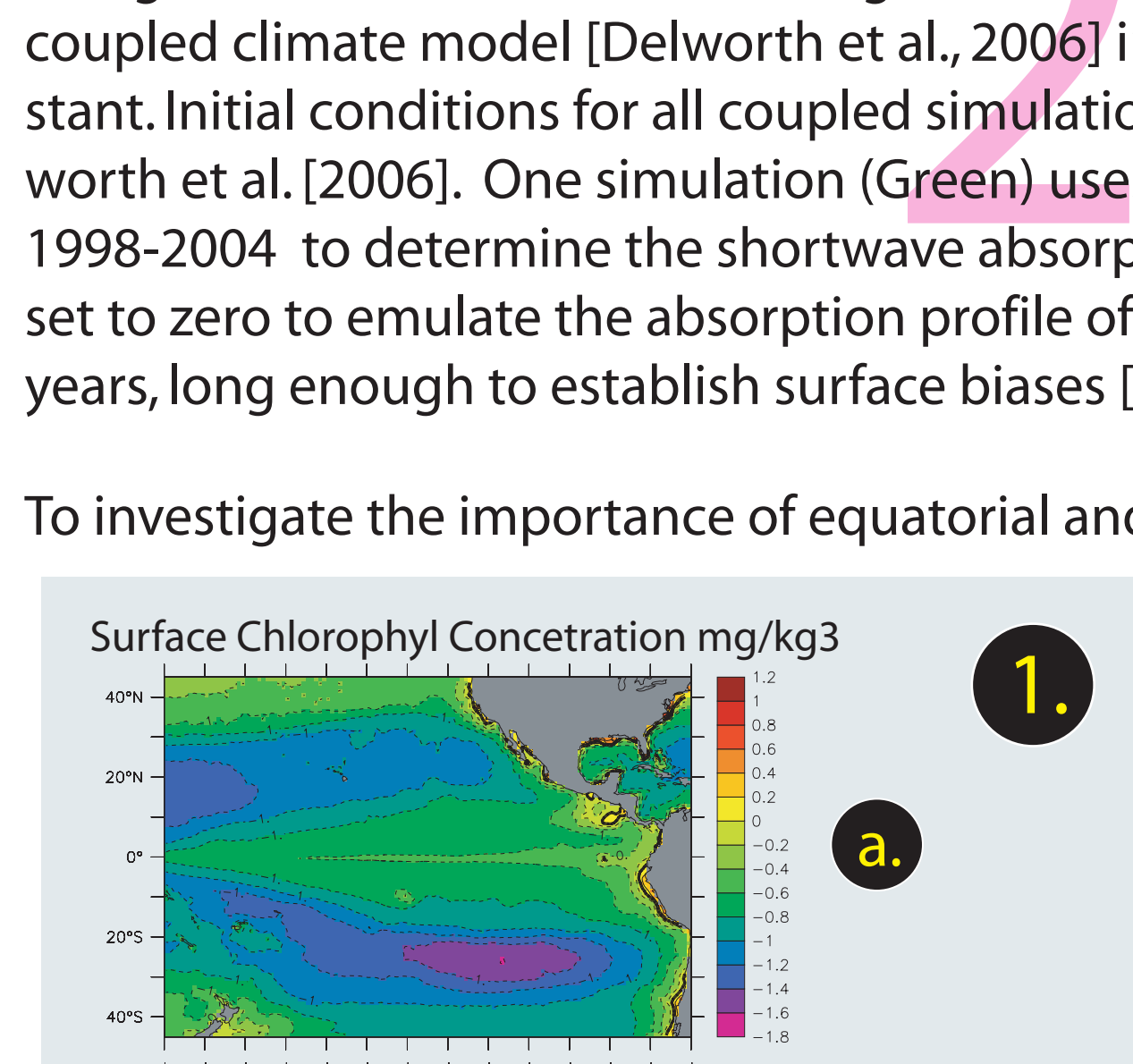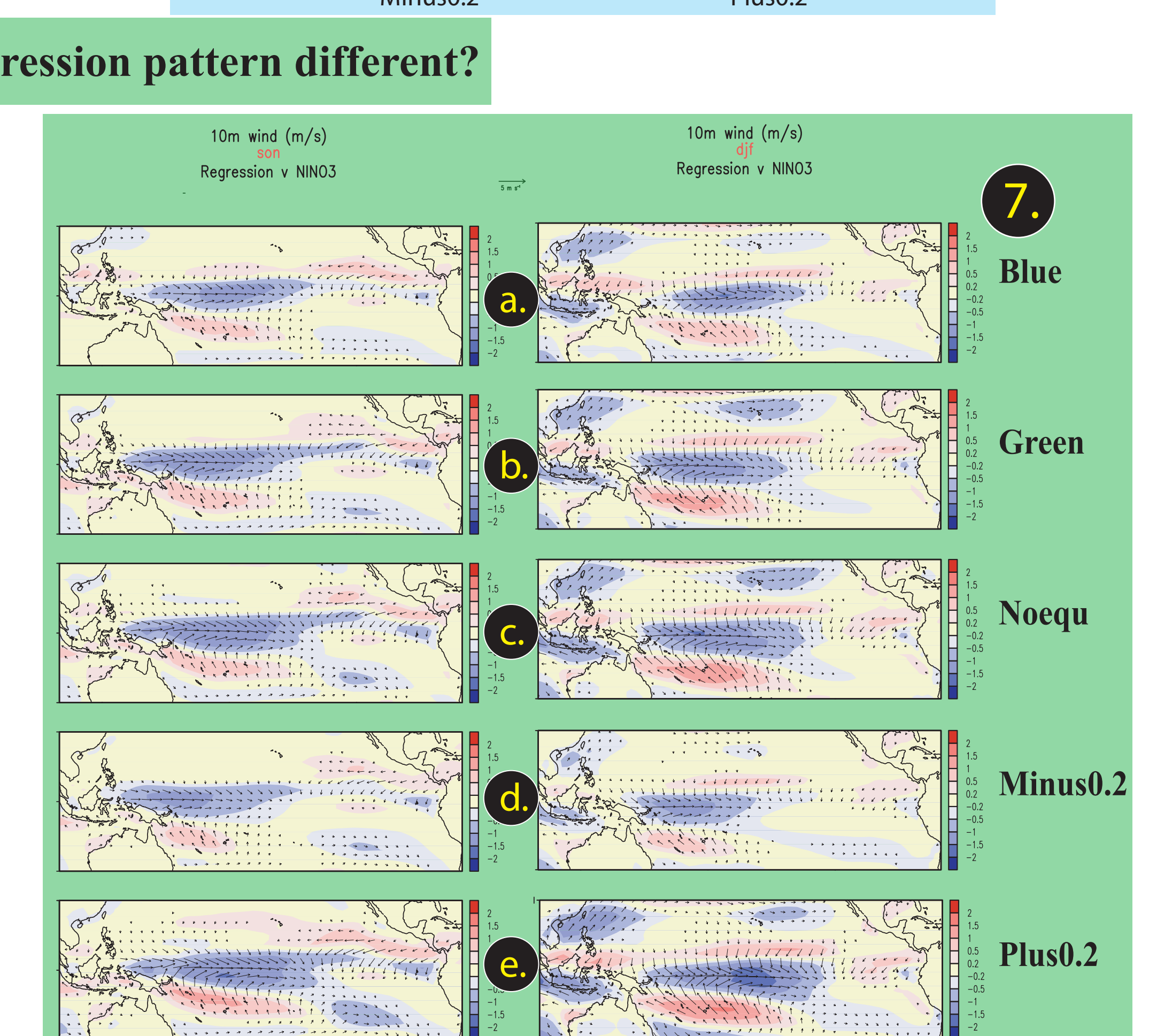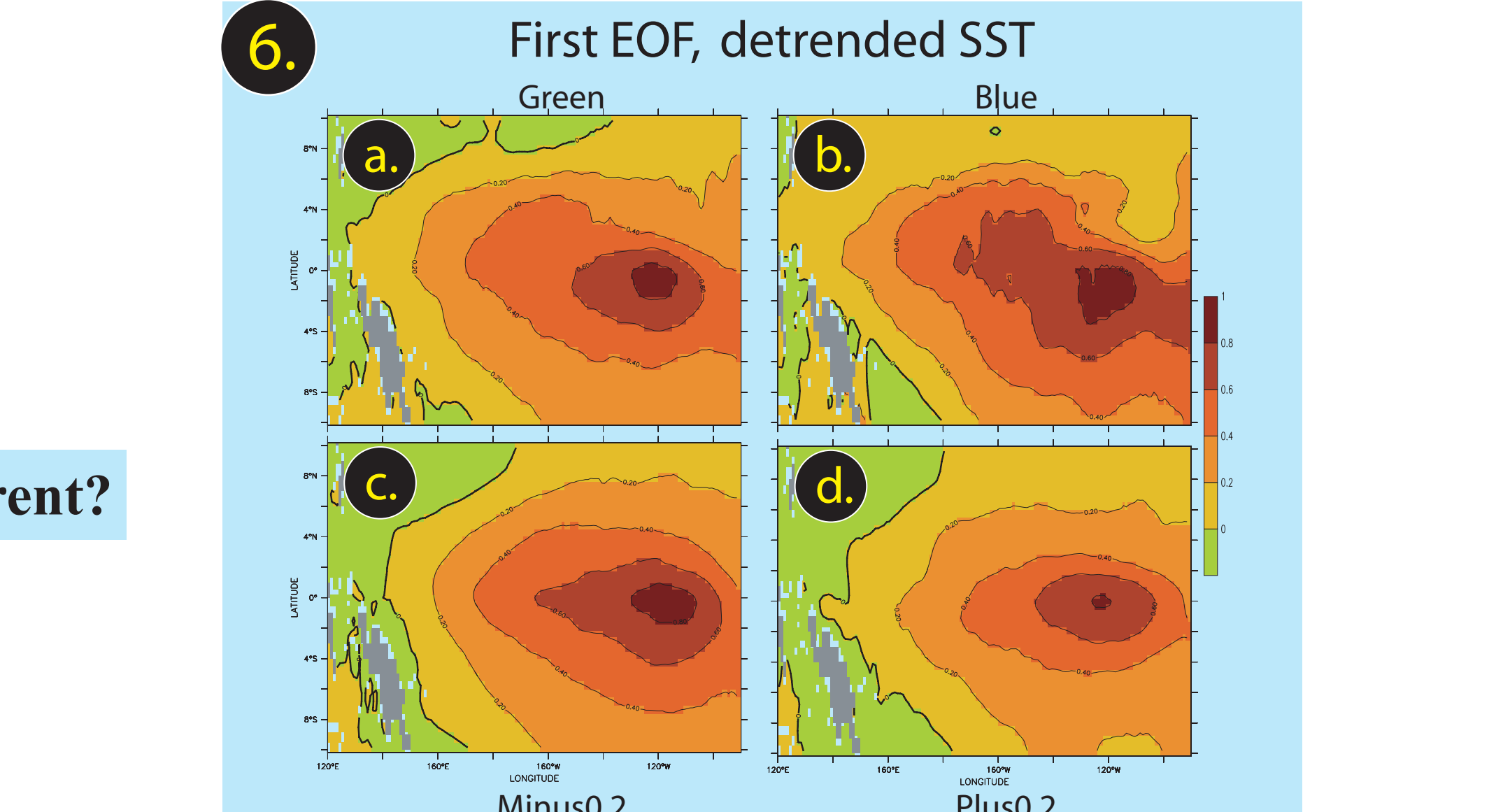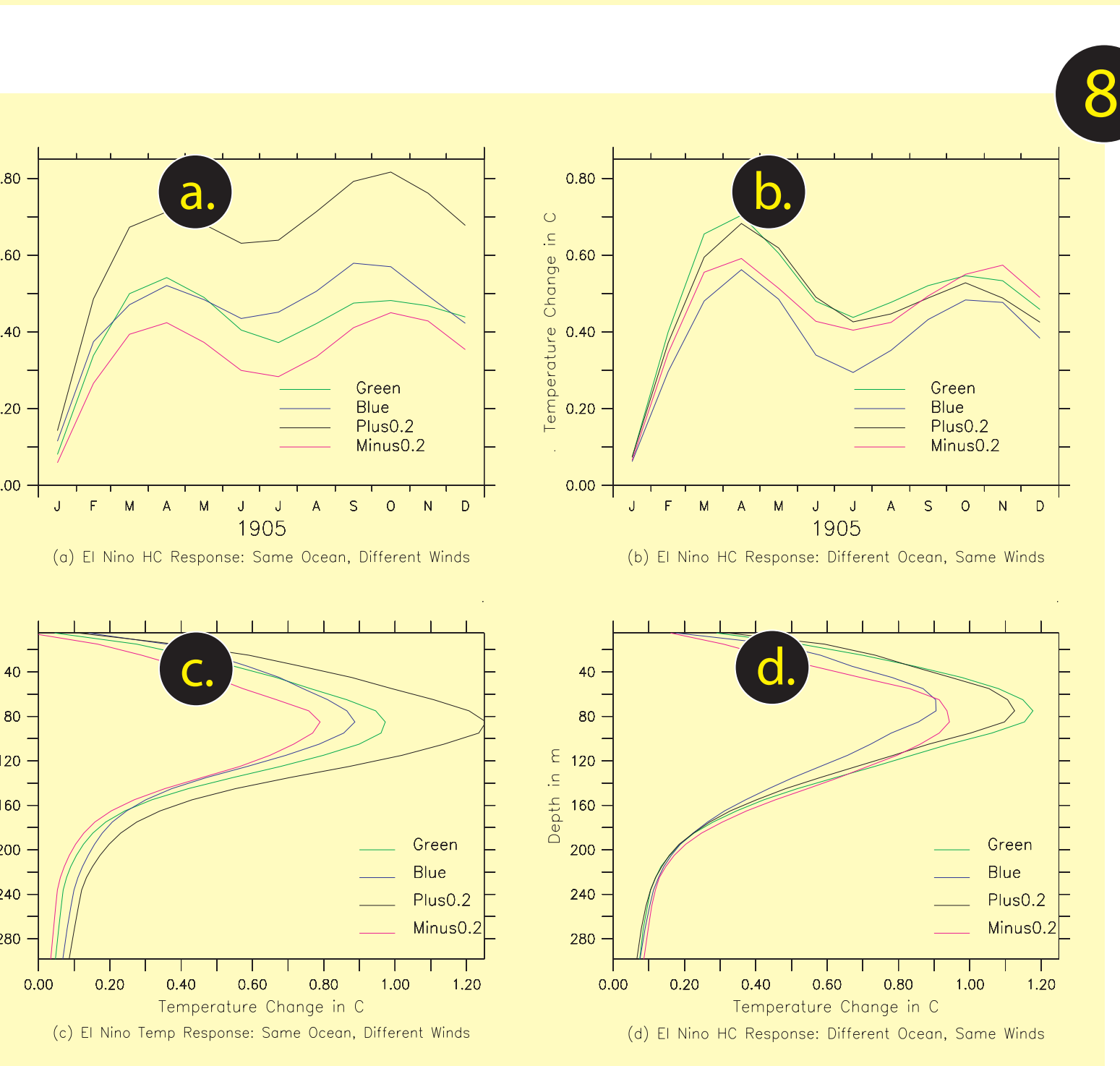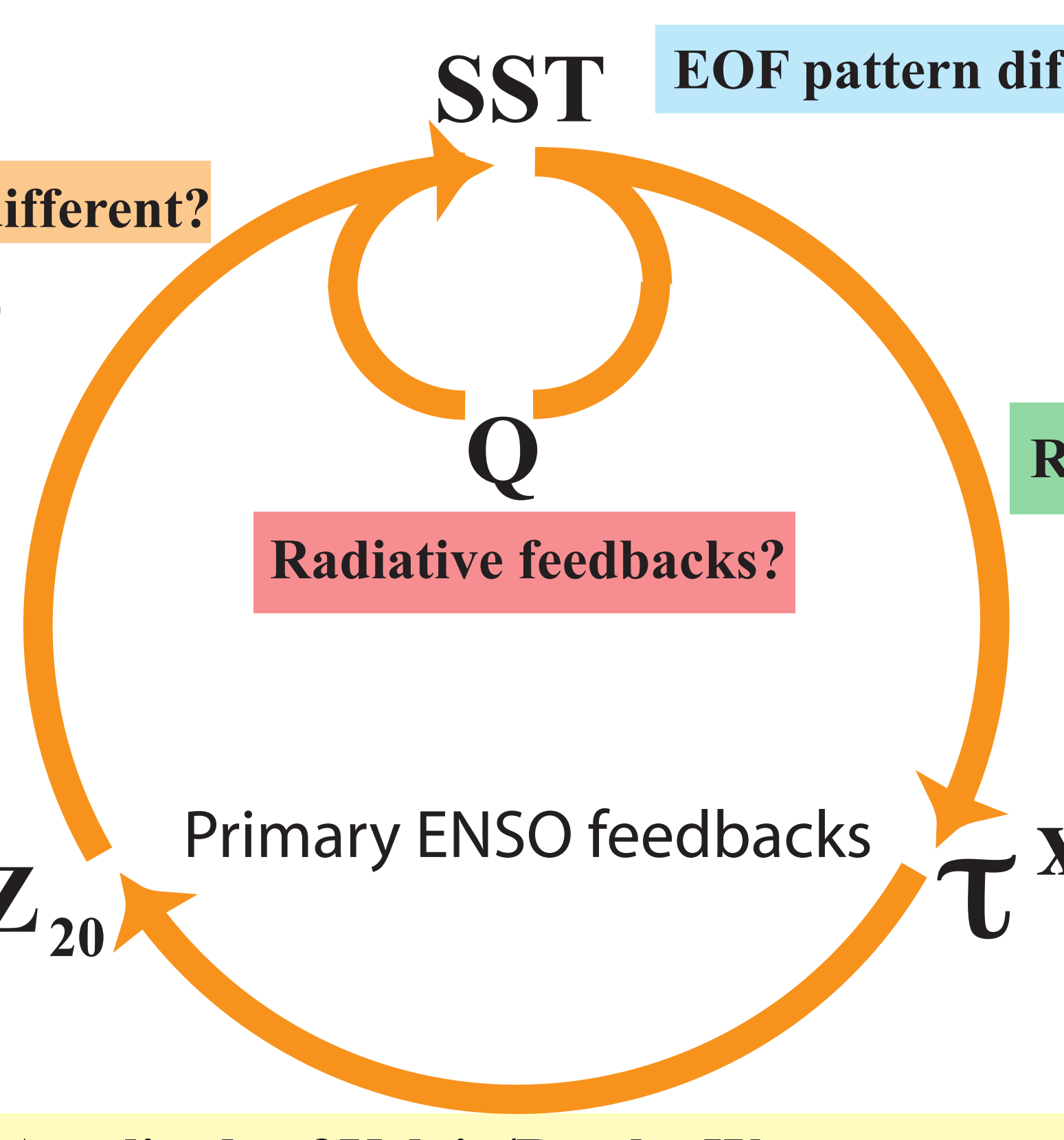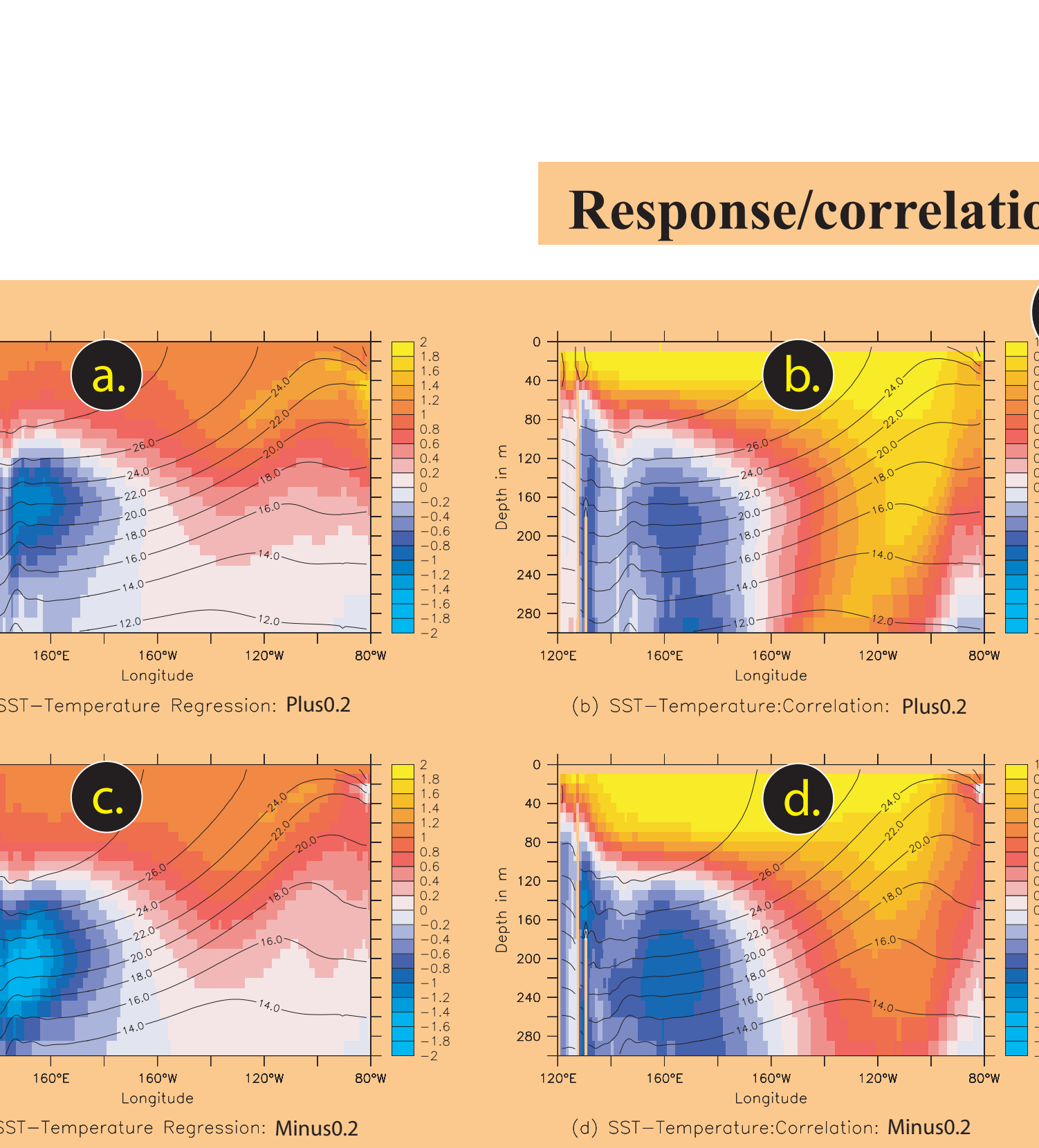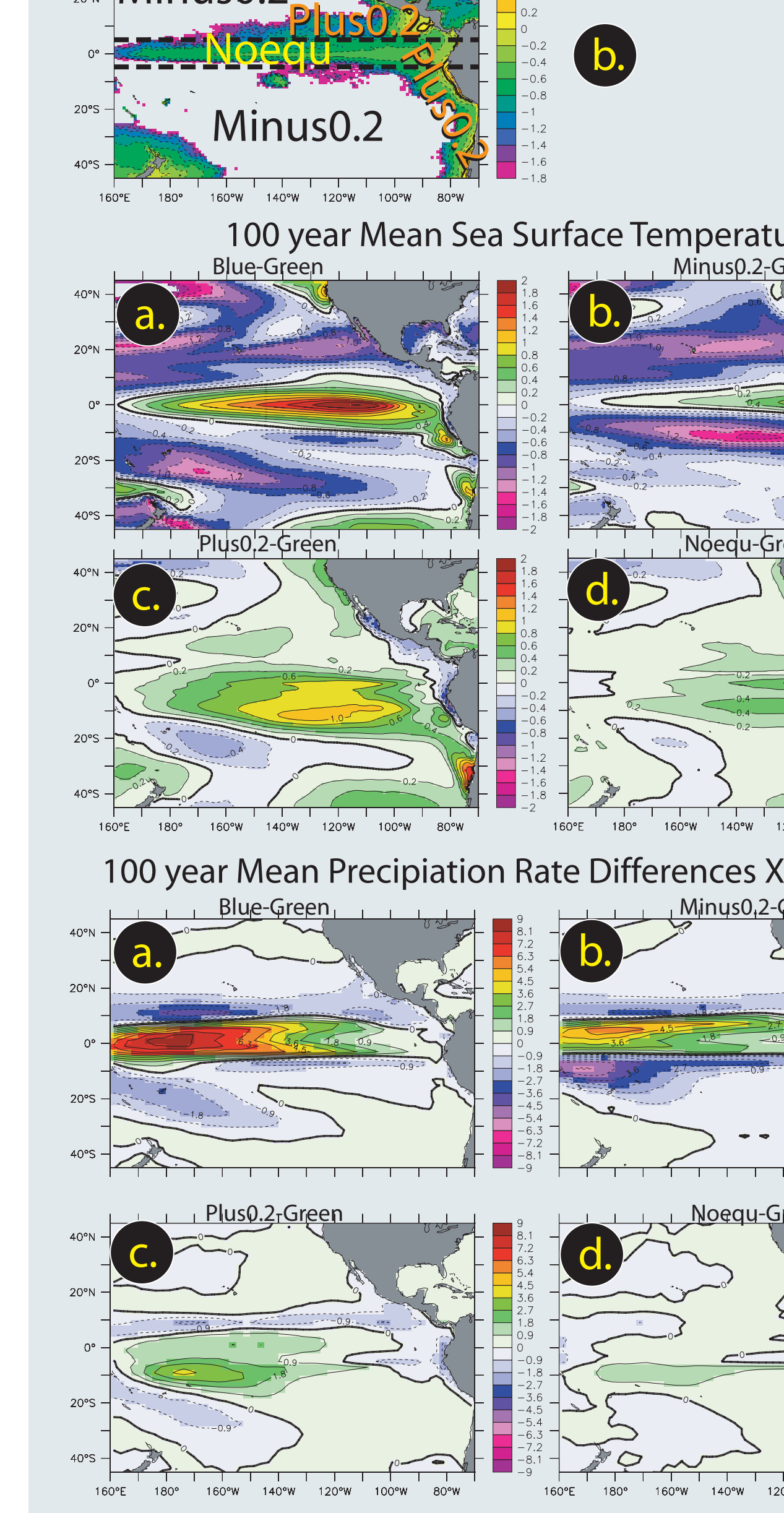
The wind response to SST anomalies is explored in Figure 7. Shown is the 10m wind speed regression versus NINO3 SST anomalies. The left column is SON. The right is DJF. Here we see a response that is consistent with the changes in variability. The experiments with larger ENSO power (Plus0.2, Green and Noequ) have a wind response with a longer fetch than Blue and Minus 0.2.

Figure 8 shows the response of heat content and the temperature profile for two suites of ocean-only experiments. In one suite (*Different Winds, Same Ocean*) the mean state of the Green ocean is used for all members and the winds are the climatology for the various coupled runs. As seen in Figure 8a and 8c, this suite highlights the different impact of the *wind stresses* in Figure 7, with the enhanced response for Plus 0.2 and smaller response for Minus 0.2 clearly visible. In the other suite (*Different Ocean, Same Winds*) the oceans are initialized with the 100 year mean states from the various coupled experiments. The atmosphere is the climatology from the Green run for all the members of the suite. As seen in Figures 8b and 8d changes in the *ocean state* are critical in explaining the diminished response in the Blue run, and act to reinforce the weaker El Nino in the Minus 0.2 run.

Feedbacks between the surface and subsurface thermal structure are explored in figure 9. Regressions and correlations between the sea surface tempreature and the temperaures in upper 300m are shown. The overall structure and response appears to be similar between Plus0.2 (strongest ENSO power) and Minus0.2 (weakest ENSO power). This shows that differences in the connection between subsurface temperatures and surface temperatures are not primarily responsible for the differences in ENSO amplitude.

• Ocean color has an impact on tropical mean state and variability.

• Increasing penetration does tend to reduce the oceanic response to wind stress, but...

• Changes in atmospheric mean state and response can overwhelm this effect.

• Different regions of ocean color (gyres vs. margins affect the atmosphere very differently!).

Ballabrera-Poy, J., R. Murtugudde, R. H. Zhang, and A. J. Busalacchi, Coupled ocean-atmosphere response to seasonal modulation of ocean color: impact on interannual climate simulations in the tropical pacific, J. Clim., 20, 353-374, 2007.
Bjerknes, J., Atmospheric teleconnections from the equatorial pacific, Mon. Wea. Rev., 97, 163–172, 1969b.
Davey, M. K., M. Huddleston, and co-authors, Stoic: a study of coupled model climatology and variability in tropical ocean regions, Clim. Dyn., 18, 403–420, 2000.
Delworth, T. L., A. Rosati, and co-authors GFDL's CM2 global coupled climate models: part 1. formulation and simulation characteristics, J. Clim., 19, 645–674, 2006.
Fedorov, A. V., P. S. Dekens, M. McCarthy, A. C. Ravelo, P. B. deMenocal, M. Barreiro, R. C. Pacanowski and S. G. Philander, The Pliocene Paradox (Mechanisms for a Permanent El Ni˜no), Science, 312, 1485-1489, 2006.
Gnanadesikan, A., J. P. Dunne, R. M. Key, K. Matsumoto, J. L. Sarmiento, R. D. Slater, and P. S. Swathi, Oceanic ventilation and biogeochemical cycling: Understanding the physical mechanisms that produce realistic distributions of tracers and productivity, Glob. Biochem. Cyc., 18, GB4010, 2004.
Gnanadesikan, A., K. W. Dixon and co-authors, GFDL's CM2 global coupled climate models-part 2: The baseline ocean simulation, J. Climate, 19, 675–697, 2005.
Hallberg, R., The suitability of large-scale ocean models for adapting parameterizations of boundary mixing and a description of a refined bulk mixed layer model, Proceedings of the 2003 Aha Hulikoa Hawaiian Winter Workshop, pp. 187–203, 2003.
Hallberg, R., A thermobaric instability of lagrangian vertical coordinate ocean models, Ocean Modelling, 8, 279-300, 2005.
Jerlov, N. G., Marine Optics, Elsevier Oceanography Series, 14, 1976.
Large, W., and S. Yeager, Diurnal to decadal global forcing for ocean and sea-ice models: the data sets and flux climatologies, NCAR Technical Note, NCAR/TN-460+STR, CGD Division of the National Center for Atmospheric Research, 2004
Lengaigne, M., C. Menkes and co-authors, Influence of the biology on the tropical Pacific climate in a coupled general circulation model, Clim Dyn, 10.1007/s00382-006-0200-2, 2007.
Lewis, M. R., M. E. Carr, G. C. Feldman, W. Esaias, and C. Mc-Clain, Influence of penetrating solar radiationon the heat budget of the equatorial Pacific ocean, Nature, 347, 543-545, 1990.
Manizza, M., C. L. Quere, A. Watson, and E. T. Buitenhuis, Bioptical feedbacks among phytoplankton, upper ocean physics and sea-ice in a global model, Geophys. Res. Lett., 32, L05603, 2005.
Marzeion, B., A. Timmerman, R. Murtugudde, and F. Jin, Biophysical feedbacks in the tropical pacific, J. Climate, 18, 58–70, 2005.
Morel, A., Optical modeling of the upper ocean in relation to its biogenous matter content (case-i waters), J. Geo. Res., 93, 10,749–10,768, 1988.
Murtugudde, R., J. Beauchamp, C. R. McClain, M. Lewis, and A. Busalacchi, Effects of penetrative radiation on the upper tropical ocean circulation, J. Climate, 15, 470–486, 2002.
Nakamoto, S., S. P. Kumar, J. M. Oberhuber, J. Ishizaka, K. Muneyama, and R. Frouin, Response of the equatorial pacific to chlorophyll pigment in a mixed layer isopycnal ocean general circulation model, Geophys. Res. Letters, 28, 2021—2024, 2001.
Rosati, A., and K. Miyakoda, A general circulation model for upper ocean simulation, J. Phys. Oceanogr., 18, 1601–1626, 1988.
Schneider, E. and Z. Zhu, Sensitivity of the simulated annual cycle of sea surface temperature in the equatorial pacific to sunlight parameterization, J. Climate, 11, 1932–1950, 1998.
Shell, K. M., S. Nakamoto and R. C. Somerville, Atmospheric response to solar radiation absorbed by phytoplankton, J. Geo. Res., 108, 1-8, 2003.
Siegel, D. A., R. R. Bidgare, and Y. Zhou, Solar radiation, phytoplankton pigments and the radiant heating of the equatorial pacific warm pool, J. Geo. Res., 100, 4885–4891, 1995.
Stramska, M., and T. D. Dickey, Phytoplankton bloom and the vertical thermal structure of the upper ocean, J. Mar. Res., 51, 819–842, 1993.
Sweeney, C., A. Gnanadesikan, S. Griffies, M. Harrison, A. Rosati, and R. Samuels, Impacts of shortwave penetration depth on large-scale ocean circulation heat transport, J. Phys. Oceanogr., 35, 1103 – 1119, 2005.
Timmerman, A., and F. Jin, Phytoplankton influences on tropical climate, Geophys. Res. Letters, 39, 10.10,129/2002GL15,434, 2002....

Acknowledgements

Figure captions

4. Mean Spectra, Nino3 SST years 0-100. s=1degC — first/last/mid/all epochs: Blue (a.), Green (b.), Minus0.2 (c.), Plus0.2 (d.). s^2 octave^{-1}

5. 100 year Mean Thermocline Depth (2N-2S) — Green, Blue, Minus 0.2, Plus 02, Noequ

6. First EOF, detrended SST — Green (a.), Blue (b.), Minus0.2 (c.), Plus0.2 (d.)

7. 10m wind (m/s) Regression v NINO3 — Blue (a.), Green (b.), Noequ (c.), Minus0.2 (d.), Plus0.2 (e.)

8. (a) SST HC Response: Same Ocean, Different Winds; (b) El Nino HC Response: Different Ocean, Same Winds; (c) El Nino Temp Response: Same Ocean, Different Winds; (d) El Nino HC Response: Different Ocean, Same Winds

9. (a) SST-Temperature Regression: Plus0.2; (b) SST-Temperature Correlation: Plus0.2; (c) SST-Temperature Regression: Minus0.2; (d) SST-Temperature Correlation: Minus0.2

1. Surface Chlorophyl Concetration mg/kg3 (a.); Minus0.2, Plus0.2, Noequ, Minus0.2 (b.)

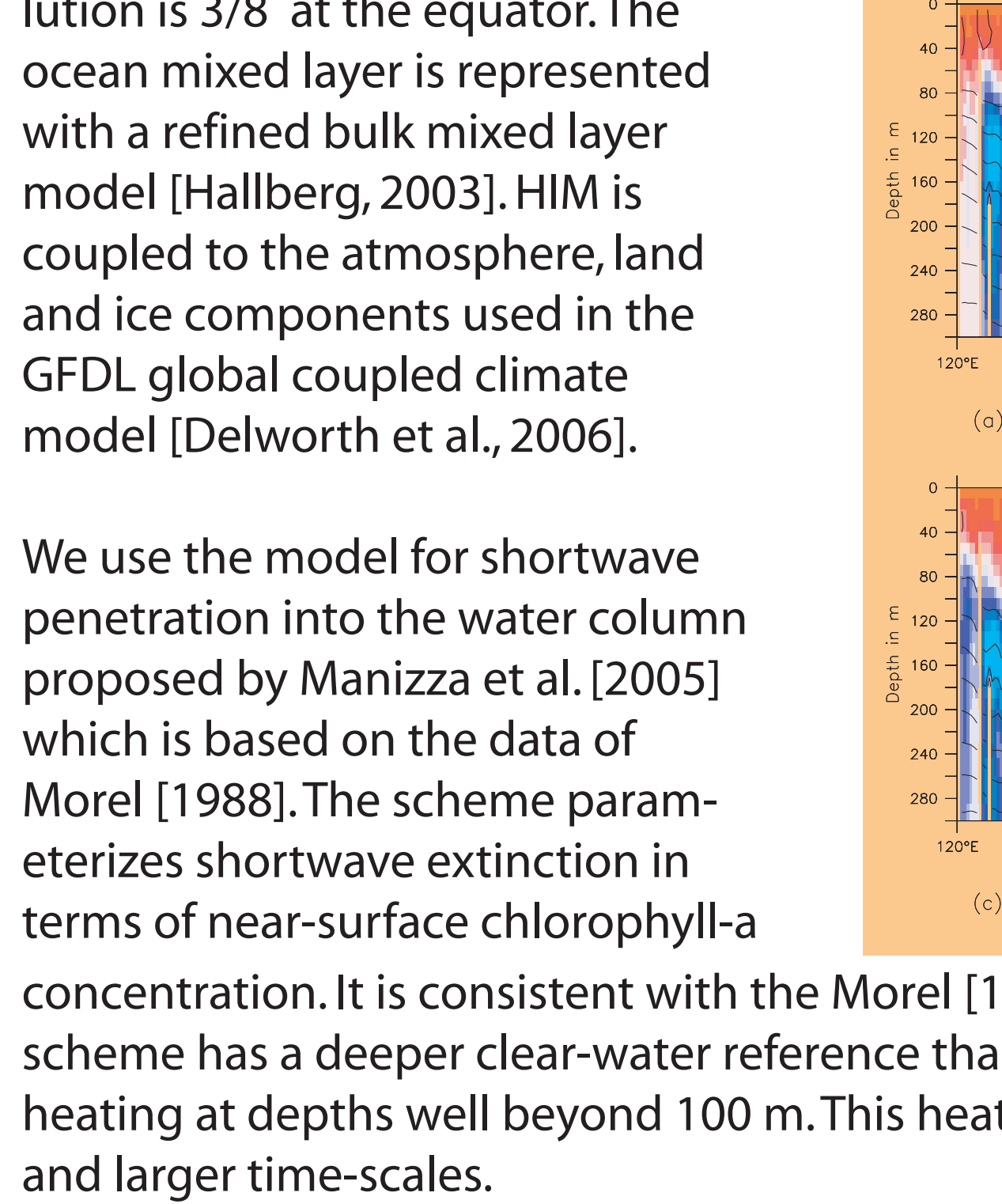**2.** 100 year Mean Sea Surface Temperature (C) — Blue-Green (a.), Minus0.2-Green (b.), Plus0.2-Green (c.), Noequ-Green (d.)

3. 100 year Mean Precipitation Rate Differences X1E5(kg/m2/s) — Blue-Green (a.), Minus0.2-Green (b.), Plus0.2-Green (c.), Noequ-Green (d.)